



# The fascinating world of mayenite ( $\text{Ca}_{12}\text{Al}_{14}\text{O}_{33}$ ) and its derivatives

Adriano Intiso<sup>1</sup> · Federico Rossi<sup>2</sup> · Antonio Proto<sup>3</sup> · Raffaele Cucciniello<sup>3</sup>

Received: 24 August 2021 / Accepted: 12 September 2021 / Published online: 21 September 2021  
© The Author(s) 2021

## Abstract

Mayenite ( $12\text{CaO}\cdot 7\text{Al}_2\text{O}_3$ ) is a mesoporous calcium aluminum oxide, with a characteristic crystalline structure. The framework of mayenite is composed of interconnected cages with a positive electric charge per unit cell that includes two molecules  $[\text{Ca}_{24}\text{Al}_{28}\text{O}_{64}]^{4+}$ , and the remaining two oxide ions  $\text{O}^{2-}$ , often labelled “free oxygen”, are trapped in the cages defined by the framework. Starting from mayenite structure several derivatives have been prepared through advanced synthetic protocols by free oxygen substitution with various anions. Mayenite and its derivatives have been intensively investigated in many applications which include catalysis (oxidation and reduction, ammonia synthesis, pinacol coupling), environmental sensors and  $\text{CO}_2$  sorbent materials. In this review, we summarize our recent results on the main applications of mayenite and its derivatives.

**Keywords** Mayenite · TCE · Catalysis · Oxidation reactions

## 1 Mayenite ( $\text{Ca}_{12}\text{Al}_{14}\text{O}_{33}$ ) structure and preparation methods

During the past decades an increasing interest has been devoted to the already known material called mayenite, mainly because of its peculiar chemical structure which is useful for a wide range of applications. Mayenite (C12A7) has the formula  $12\text{CaO}\cdot 7\text{Al}_2\text{O}_3$  and it is a mesoporous calcium aluminate as shown in the  $\text{CaO}\text{--}\text{Al}_2\text{O}_3$  phase diagram. Discovered in Mayen (Germany) as a rare mineral, mayenite is mainly found as a component of alumina cements. Mayenite structure has a positively charged lattice framework  $[\text{Ca}_{24}\text{Al}_{28}\text{O}_{64}]^{4+}$  per unit cell that includes two molecules and twelve cages with a free space of 0.4 nm in diameter (Cucciniello et al. 2017a). The chemical formula for the unit

cell may be represented as  $[\text{Ca}_{24}\text{Al}_{28}\text{O}_{64}]^{4+} \cdot 2\text{O}^{2-}$  and it has a body centered cubic crystal structure belonging to the  $I\text{-}43d$  space group with  $a = 11.989 \text{ \AA}$  and  $Z = 2$ . The two oxide ions  $\text{O}^{2-}$ , namely “free oxygen”, are trapped in the cages defined by the framework satisfying the overall electroneutrality condition. Due to the space confinement, the guest species are limited to mono or diatomic such as  $\text{O}^{2-}$ ,  $\text{O}^-$ ,  $\text{O}_2^-$ ,  $\text{O}_2^{2-}$ ,  $\text{OH}^-$  (Ruszak et al. 2007; Dong et al. 2013). Mayenite derivatives were obtained by exchanging the  $\text{O}^{2-}$  anions with other active species, such as  $\text{OH}^-$ ,  $\text{F}^-$  and  $\text{Cl}^-$ ,  $\text{O}_2^-$ , electrons,  $\text{S}^{2-}$ ,  $\text{CN}^-$  and  $\text{H}^-$  (Hayashi et al. 2002a,b,2005,2007,2014a; Kitano et al. 2012; Schmidt et al. 2014; Eufinger et al. 2015; Proto et al. 2015).

As shown in Fig. 1, the important role played by mayenite alongside the academic community is also confirmed by the publications trend: according to the Scopus<sup>®</sup> database, during the past 10 years there has been a sensible increase in the number of publications about the synthesis, characterization and applications of mayenite and its derivatives.

Several methods have been reported for the mayenite synthesis, which involves the use of low-cost starting materials (aluminum and calcium precursors, mainly nitrates and hydroxides). The preparation of mayenite plays an important role in determining the properties of the material, among them surface area and concentration of the oxide anion in the nanocages. This approach is able to modulate the chemical-physics properties of this functional material and

---

Author Raffaele Cucciniello received the “Alfredo Di Braccio 2020” award from the Accademia Nazionale dei Lincei in Rome.

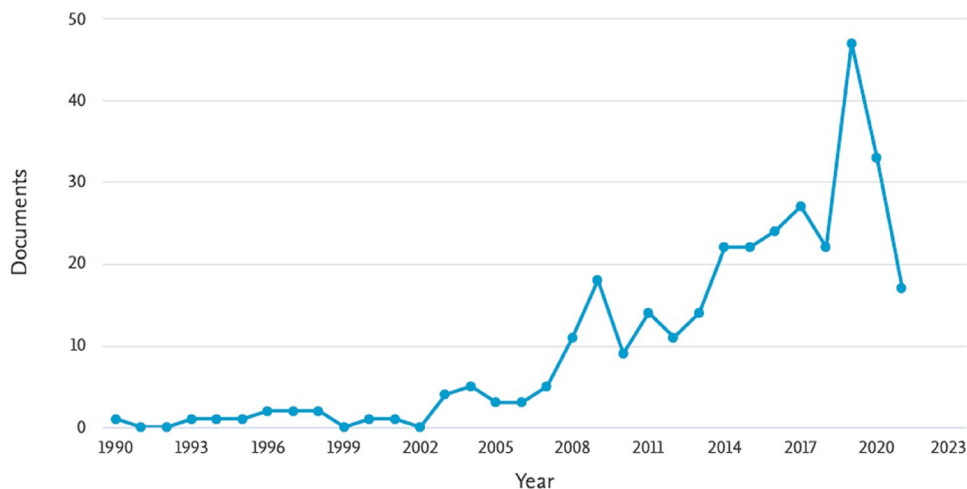
✉ Raffaele Cucciniello  
rcucciniello@unisa.it

<sup>1</sup> Lamberti Design SRL, Via G. Vitale 58,  
84013 Cava de' Tirreni, SA, Italy

<sup>2</sup> Department of Earth, Environmental and Physical Sciences –  
DEEP Sciences, University of Siena, Pian dei Mantellini 44,  
53100 Siena, Italy

<sup>3</sup> Department of Chemistry and Biology “Adolfo  
Zambelli”, University of Salerno, Via Giovanni Paolo II,  
132-84084 Fisciano, SA, Italy

**Fig. 1** Trend of the peer-review manuscripts per year which contain “mayenite” in abstract, keywords and title. Adapted from Scopus® (accessed 6/2021)



consequently the potential application field. Here, we discuss the most common preparation methods.

Mayenite can be prepared by following the ceramic method reported by Li et al. (2011), using a stoichiometric mixture of  $\text{Ca}(\text{OH})_2$  and  $\text{Al}(\text{OH})_3$  in distilled water. The mixture is grounded under magnetic stirring for 4 h at room temperature, afterwards, is placed in a stainless-steel autoclave at 150 °C for 5 h. The obtained solid is filtered and dried at 120 °C overnight, crushed into fine powder and finally placed into a furnace at 1000 °C in air for 4 h. This material generally shows a very low surface area ( $< 10 \text{ m}^2 \text{ g}^{-1}$ ) and a low reducibility ( $0.45 \text{ mmol H}_2 \text{ g}^{-1}$  of mayenite), determined by means of temperature programmed reduction (TPR), corresponding to a poor oxygen anion concentration in the nanocages (Intiso et al. 2019a).

Mayenite can also be synthesized by following the hydrothermal method (Li et al. 2011). In this case, a stoichiometric amount of  $\text{Ca}(\text{OH})_2$  and  $\text{Al}(\text{OH})_3$  is mixed with distilled water. The mixture is ground to powder under magnetic stirring for 4 h at room temperature; afterwards, it is placed in a stainless-steel autoclave at 150 °C for 5 h. The recovered solid is filtered and dried at 120 °C for 8 h, crushed into fine powder and finally placed into a furnace at 600 °C in air for 4 h. With respect to ceramic, mayenite prepared by the hydrothermal procedure shows a higher surface area ( $36 \text{ m}^2 \text{ g}^{-1}$ ) and a higher reducibility ( $1.19 \text{ mmol H}_2 \text{ g}^{-1}$ ) (Intiso et al. 2019a).

Another widely employed synthesis method is the citrate-sol-gel procedure, carried out according to the method proposed by Ude and coworkers starting from calcium nitrate tetrahydrate,  $\text{Ca}(\text{NO}_3)_2 \cdot 4\text{H}_2\text{O}$ , and  $\text{Al}(\text{NO}_3)_3 \cdot 9\text{H}_2\text{O}$  in distilled water (Ude et al. 2014). The solution is heated at 60 °C, then 5 g of citric acid ( $\text{C}_6\text{H}_8\text{O}_7$ ) are added. The citrate-nitrate mixture is heated and vigorously stirred at 90 °C until a gel is formed (about 12 h). The resulting gel is placed in a drying oven at 120 °C until a cake-like structure

is produced. The solid is then crushed into fine powder and finally calcined at 1000 °C in air for 4 h. Sol-gel mayenite reports a surface area of  $14.9 \text{ m}^2 \text{ g}^{-1}$  and reducibility of  $1.16 \text{ mmol H}_2 \text{ g}^{-1}$  (Intiso et al. 2019a). A small drawback of this procedure is that  $\text{H}_2$  uptake can be affected by the presence of nitrate impurities, sometimes left during the preparation.

To increase the surface area and the concentration of oxygen anions in the nanocages, polymer-assisted combustion preparation of mayenite has been recently reported by our research group (Intiso et al. 2019b). Intiso et al. showed that the use of polymethylmethacrylate (PMMA) was able to increase the surface area of the mayenite up to  $47.1 \text{ m}^2 \text{ g}^{-1}$ . Herein, mayenite was prepared by adding different amounts of polymer (10, 20% *w/w*) to a stoichiometric mixture of  $\text{Ca}(\text{OH})_2$  and  $\text{Al}(\text{OH})_3$  in distilled water. The mixture was ground to powder under magnetic stirring for 4 h, then placed in a teflon-lined stainless-steel autoclave at 150 °C for 5 h. The solid was recovered by filtration and dried at 120 °C for 8 h. After, the solid was calcined to obtain the mayenite phase following an heating cycle of 2.6 °C/min from RT up to 500 °C in  $\text{N}_2$  atmosphere, T was kept constant at 500 °C for 4 h in  $\text{N}_2$  to eliminate PMMA, then raised again at 1.7 °C/min from 500 to 600 °C in air atmosphere and finally kept at 600 °C in air for 4 h.

Recently, new synthetic approaches have been investigated to produce porous mayenite powder at milder conditions, especially at lower temperatures as well as modified sol-gel route in the presence of oxalic acid (Rashad et al. 2016) and an assisted solution combustion synthesis (SCS) (Da Fumo et al. 1996). Herein, mayenite was prepared via a single fuel approach by mixing Al and Ca nitrates with urea or glycine followed by an annealing step at high temperatures (Raab and Poellmann 2011). Recently, Gaigneaux reported the direct formation of pure crystalline mayenite with a high specific surface via the solution combustion

technique using glycine and  $\beta$ -alanine as fuels (Meza-Trujillo et al. 2019). Furthermore, the addition of oxalic acid as a pore generator was also discussed. The mayenite textural properties were tuned by varying the calcination temperature making possible the formation of porous mayenite from temperatures as low as 275 °C, reaching a remarkable specific surface area of 74 m<sup>2</sup> g<sup>-1</sup> at 400 °C and displaying a large pore volume of 0.3 cm<sup>3</sup> g<sup>-1</sup>.

Recently, ultrasound-assisted approach was successfully applied for the synthesis of mayenite from calcium and aluminum hydroxides and then subsequently impregnated with Ni by the wet impregnation method. Ultrasound promoted an effective dispersion of the precursors in a short time of 10 min leading to a high conversion to mayenite after calcination at 1200 °C. Ultrasound treatment also had a positive effect on Ni impregnation, increasing the dispersion of the metal in the support and leading to a stronger interaction of nickel-containing species with mayenite support (Manera et al. 2020).

## 2 Mayenite as active support/catalyst

### 2.1 VOCs' oxidation and steam-reforming

Volatile Organic Compounds (VOCs) are emitted from a wide range of outdoor and indoor sources, such as transport and industrial processes as well as from household products (Heck et al. 2012; Scirè and Liotta 2012). These compounds have been identified as components of the photochemical smog and responsible for ground-level smog formation, tropospheric ozone formation, stratospheric ozone depletion and climate change (Amann and Lutz 2000).

Several techniques have been developed for the destruction of these contaminants from gases (Aranzabal et al. 2014; Tomatis et al. 2016). Catalytic oxidation represents an economically effective alternative for the oxidation of VOCs into CO<sub>2</sub>, water, and other less harmful products (Liotta 2010). Catalysts allow to work at much lower temperatures (250–500 °C) than thermal incineration, which results in the following two main advantages: lower energetic and operating costs, and reduction of undesirable by-products formation.

Generally, catalytic activity is evaluated by monitoring the conversion as a function of the temperature (also known as light-off curve) (Aranzabal et al. 2014).  $T_{50}$  and  $T_{90}$  (temperatures at which 50% and 90% conversion is reached) are commonly used to evaluate catalyst activity.

Catalyst activity, selectivity and stability are fundamental parameters to address the choice of an efficient material for the abatement of VOCs. Several factors such as water and other VOCs as hydrogen-supplying compounds can influence catalytic activity and product (Aranzabal et al.

2014). Catalyst deactivation is due to several mechanisms that occur depending on the type of the reaction. The most important are as follows: coke deposition, poisoning, volatilization of active phase and thermal degradation (Aranzabal et al. 2014).

In this scenario, mayenite was successfully employed as an active support for catalysts (or as a catalyst material itself) for VOCs' destruction. Furthermore, the ability of storing oxygen ions in the nanocages is a unique property of mayenite and several works show its application in catalytic processes as an oxidant species (Vernoux et al. 2013). The most promising characteristic of mayenite to be exploited for catalysis is that the encaged oxygen species can migrate between the surface and the bulk and they can be gradually released at elevated temperatures or stored (Lacerda et al. 1988; Teusner et al. 2015, 2016). Therefore, the reported catalytic activity properties of mayenite have often been associated with its strong oxidation ability and have been exploited for applications as oxidation catalyst or active support for metals in oxidation reactions.

Indeed, the use of mayenite as substrate for Ni catalyst was reported for biomass tar steam reforming in a fixed bed reactor using toluene as tar destruction model compound. 1% Ni on mayenite shows excellent performances either in absence and presence of H<sub>2</sub>S. Moreover, Ni/Ca<sub>12</sub>Al<sub>14</sub>O<sub>33</sub> showed excellent sustainability against coke formation due to the “free oxygen” in the catalyst. O<sub>2</sub><sup>2-</sup> and O<sub>2</sub><sup>-</sup> inhibit Ni poisoning due to the sulphur incorporation in the cages (Li et al. 2009).

Hosono et al. have investigated the partial oxidation of methane to CO and H<sub>2</sub> over mayenite-promoted metals such as Ni, Co, Pt, Rh and Ru (Yang et al. 2004). On Ni, Pt and Pd/C12A7, this reaction readily happened at temperatures as low as 500 °C and attained thermodynamic equilibrium. Mayenite without any metal catalyst shows good performance in the partial oxidation of methane as well. Furthermore, ethane and ethene were also formed at temperatures higher than 650 °C (10% selectivity at 800 °C) due to the existence of active oxygen (O<sup>-</sup>, O<sup>2-</sup>, O<sub>2</sub><sup>2-</sup>) in C12A7 which readily activated methane into radicals and caused their coupling. When mayenite was promoted by Ni, Pt and Pd, partial oxidation of methane into CO and H<sub>2</sub> readily proceeded even at 500 °C.

The role of mayenite as an active catalyst for the VOCs oxidation was investigated by Fujita et al. (2006). They synthesized and tested different calcium aluminosilicate (Ca<sub>12</sub>Al<sub>14</sub>O<sub>33</sub> (C12A7), Ca<sub>12</sub>Al<sub>14</sub>Si<sub>2</sub>O<sub>34</sub> (C12A6) and Ca<sub>12</sub>Al<sub>10</sub>Si<sub>4</sub>O<sub>35</sub> (C12A5)) for the total oxidation of propylene and benzene. Mayenite was found to be the most active catalyst for the oxidation of both pollutants at 575 °C. Both CO and CO<sub>2</sub> were formed from the oxidation of benzene, whereas only CO<sub>2</sub> was formed from the oxidation of propylene. The authors attributed the major activity in oxidation

reaction to  $O_2^-$  instead of  $O_2^{2-}$ . In fact, contrary to  $O_2^{2-}$ , the  $O_2^-$  signal was found to disappear upon reacting with hydrogen and to appear again by reacting with oxygen. This preferential disappearing/appearing behavior suggests the higher reactivity of  $O_2^-$  species for the oxidation of hydrocarbons.

The authors pointed out that without catalyst (only fragmented quartz glass packed), the oxidation reaction of propylene started around 600 °C, while, in the presence of the catalyst, the same reaction was observed at 400 °C. Same results were observed for benzene oxidation; also in this case, the presence of calcium aluminosilicate catalyst allowed to reach lower temperature for the total oxidation of the pollutant.

Zhang and co-workers reported the use of mayenite  $12MO \cdot 7Al_2O_3$  ( $M = Ca, Sr$ ) as active support for  $La_{0.8}Sr_{0.2}MnO_3$  (LSM) cordierite monoliths catalyst, to improve its thermal stability (Zhang et al. 2014). The catalytic performances of the synthesized materials were evaluated for methyl methacrylate combustion.

LSM/ $C_{12}A_7$  shows the best activity among the three monoliths.  $T_{98}$  of MMA on the LSM/ $C_{12}A_7$  is about 270 °C, while  $T_{98}$  on the LSM/ $Al_2O_3$  is 305 °C and on the LSM/CH,  $T_{98}$  above 340 °C. Thus, the  $C_{12}A_7$  support obviously improves both the physicochemical properties and the catalytic activity of LSM monolith and it is a better supporting material for LSM monolith with respect to  $\gamma-Al_2O_3$ . These results are due to the mayenite capability to enhance the dispersion of LSM and to inhibit the interaction between LSM and cordierite or  $\gamma-Al_2O_3$ ; both crystal structure and surface morphology of LSM phase can thereby be stable on the mayenite surface even at high temperature (up to 1050 °C).

Phenol, used as a tar model compound in a laboratory-scale fixed bed reactor, steam-reforming was carried out by Wang et al. (2020). The Ni/CaO– $Ca_{12}Al_{14}O_{33}$  prepared by calcination–hydration method exhibited a higher hydrogen production. The optimum operative condition for the process was obtained at the temperature of 650 °C with S/C ratio of 3.0. Under this condition, the maximum  $H_2$  concentration of 69.75% was achieved for Ni/CaO– $Ca_{12}Al_{14}O_{33}$ . The corresponding  $H_2$  yields were  $1.61 \text{ Lg}^{-1}$  and  $1.45 \text{ Lg}^{-1}$ . However, a rapid deactivation of the Ni/CaO– $Ca_{12}Al_{14}O_{33}$  catalytic sorbents occurred during the cyclic tests due to the carbon deposition on the catalyst surface.

Scaccia et al. reported the dry reforming of methane over 15 wt% Ni/CaO– $Ca_{12}Al_{14}O_{33}$  catalyst in a microreactor in the temperature range 600–800 °C under atmospheric pressure, at a weight hourly space velocity (WHSV) of  $120 \text{ Lg}^{-1} \text{ h}^{-1}$  and by time on stream of 12 h for producing synthesis gas. The presence of CaO avoids the formation of coke deposit onto the catalyst surface increasing the reaction productivity (Scaccia et al. 2021).

Mayenite was also used in combination with iron catalyst as in the work of Zamboni and coworkers where Fe/CaO/

Mayenite acts as catalyst in toluene steam reforming. Fe promotes the  $H_2$  production, whereas CaO/mayenite simultaneously captures  $CO_2$  during several cycles of carbonation–decarbonation (Zamboni et al. 2015). Moreover, the presence of the  $Ca_{12}Al_{14}O_{33}$  phase improves the CaO surface properties and stabilizes the  $CO_2$  sorption capacity during several cycles. The Fe/CaO/ $Ca_{12}Al_{14}O_{33}$  bi-functional material showed the best properties for the simultaneous toluene steam reforming at low temperature and  $CO_2$  capture at 700 °C evaluated as a good compromise for  $CO_2$  sorption and biomass gasification. The same authors have also reported the use of olivine (mixture of  $Mg_2SiO_4$  and  $Fe_2SiO_4$ ) catalyst supported on CaO or CaO– $Ca_{12}Al_{14}O_{33}$  used as  $CO_2$  sorbent phases in biomass reforming of hydrogen production in a fast internal circulating fluidized bed biomass gasifier (Zamboni et al. 2014). The enhancement of catalytic activity in tar conversion for these bi-functional materials compared to olivine was demonstrated and attributed to the presence of well-dispersed iron oxides and the high content of sorbent on the olivine surface.

## 2.2 Oxidation of chlorinated compounds

Among VOCs, Cl-VOCs are organochlorinated compounds that present widespread applications in industry and show high toxicity and stability in the environment. TCE is a chlorinated solvent that belongs to the class of dense non-aqueous phase liquids (DNAPLs) pollutants (Liotta 2010; Rossi et al. 2015). It is a colorless non-flammable liquid, hardly soluble in water with a sweet smell. Very recently, it has been classified into group 1 compounds by the IARC (International Agency for Research on Cancer), indicating that it is certainly carcinogenic to humans (IARC Working Group on the Evaluation of Carcinogenic Risks to Humans 2014). Catalytic oxidation of TCE represented a very efficient technique to operate at lower temperatures (200–600 °C) with a drastic reduction of energetic costs with respect to classic thermal incineration methods. In the past few years, several works reported the preparation of catalysts able to oxidize TCE. In particular, metal oxides and supported noble metals have been described as active catalysts, but they also have some limitations due to the formation of toxic by-products, such as chlorine and perchloroethylene (López-Fonseca et al. 2004; Divakar et al. 2011; Romero-Sáez et al. 2016).

Blanch-Raga and coworkers synthesized and used hydrotalcite-like compounds to host metal catalysts, such as Mg(Fe/Al), Ni(Fe/Al) and Co(Fe/Al), showing good performances for the TCE oxidation, mainly due to the presence of  $O_2^-$  and  $O_2^{2-}$  sites that enhance the catalytic productivity. At the same time, the authors observed the formation of several by-products ( $HCl$ , PCE and  $Cl_2$ ) (Blanch-Raga et al. 2014).

Acid zeolites have also been evaluated, showing a good activity but suffering a deactivation process due to chlorine

attack and coke deposition to the active sites (Aranzabal et al. 2012).

In order to improve the catalyst activity and selectivity towards less harmful products, a combination of transition metal and zeolite has been proposed by several authors. Blanch-Raga et al. prepared and tested Cu- and Co-doped beta zeolites in the TCE oxidation (Blanch-Raga et al. 2016).

The results showed that Cu-zeolite synthesized by ion exchange was the best catalyst in terms of activity and selectivity, due to the combination of the zeolite acidic properties with the metal redox properties.

Similarly, Golabek et al. reported the activity of different Cerium- BEA zeolites for the TCE oxidation (Gołabek et al. 2019). It was shown that highly developed mesopore surface area, well-dispersed cerium species and a high number of Brønsted sites result in a higher activity. Moreover, the hierarchical materials with a higher density of hydroxyls showed higher yields to HCl while the formation of chlorine was avoided.

In this context, many efforts are directed towards the research of new catalysts able to oxidize TCE with high productivity, selectivity and recyclability. The use of noble or transition metal-free catalysts has to be preferred to avoid the metals depletion and the high costs for their recovery at the end of the material life-cycle. In the past few years, our research focused on the use of mayenite as an active catalyst for the total oxidation of trichloroethylene (TCE) (Cucciniello et al. 2017a).

We reported the use of undoped mayenite as catalyst for the oxidation of gaseous TCE. The catalyst was synthesized by using a hydrothermal method and TCE oxidation was carried out in a stainless-steel fixed bed reactor. Figure 2 reports TCE conversion over mayenite catalyst.

As can be seen, the catalytic oxidation of TCE started at  $T > 200$  °C, and the conversion drastically increased with the

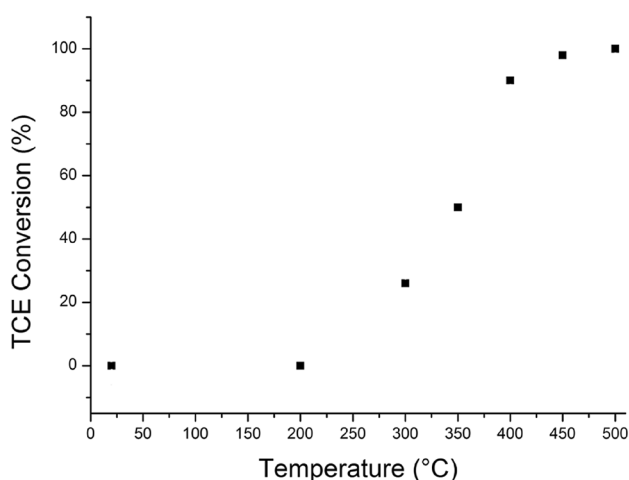


Fig. 2 TCE oxidation over mayenite catalyst

temperature, and it reached the values of 75% and 90% for a temperature of 400 °C and 450 °C, respectively. Furthermore, the results showed that TCE was totally converted in CO<sub>2</sub> and CO and the released chlorine was incorporated in the mayenite structure. As mentioned in the introduction, the high performance of the catalyst is related to its oxidative properties due to the presence of O<sub>2</sub><sup>-</sup> and O<sub>2</sub><sup>2-</sup> anion sites that favors the total oxidation of TCE and avoid the formation of coke.

Later, we investigated how metal loading can improve mayenite activity. In particular, several mayenite-based catalysts loaded with iron (Fe/mayenite) were prepared and tested for TCE oxidation (Fig. 3).

As can be seen, mayenite loaded with the maximum amount of Fe (2.0%) was found to be the best catalyst synthesized for the TCE oxidation reaction. This result was related to the strong interaction between the transition metal with the mayenite framework, which enhanced the catalytic performance of the material (Cucciniello et al. 2019).

Fe/mayenite was found to be more active and stable than the pure material for TCE oxidation, maintaining the same selectivity. This result was interpreted as the synergistic effect of the metal and the oxo-anionic species present in the mayenite framework, thus promoting TCE oxidation, while avoiding catalyst deactivation. The selectivity was also evaluated, and the results showed that the presence of Fe on the mayenite structure did not alter the selectivity of the reaction, and the main products observed were CO<sub>2</sub>, CO and HCl. Stability test was also performed for 2.0% Fe/mayenite, in comparison with pure mayenite, by using the catalyst for several hours (12 h) at operative conditions ( $T = 460$  °C, 1700 ppm TCE, GHSV = 6000 h<sup>-1</sup>, 0.8 g of catalyst). The results showed that the addition of iron in the mayenite framework allowed to improve the stability of the

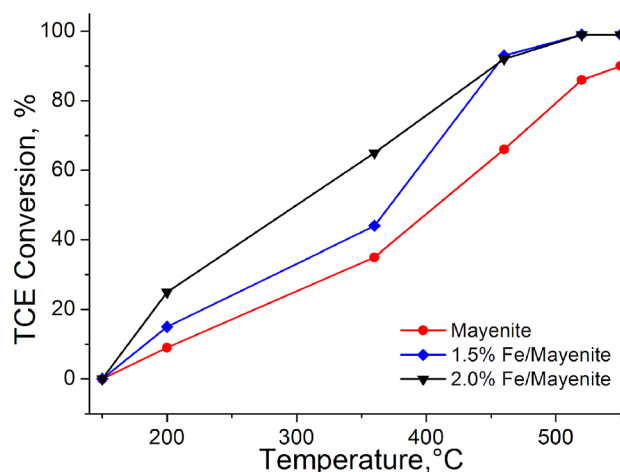


Fig. 3 TCE conversion for Mayenite (circle), 1.5% (square) and 2.0% (triangle) Fe/Mayenites



material. Indeed, a partial deactivation of 2.0% Fe/mayenite was observed only after 12 h, whereby pure mayenite was totally deactivated after 6 h.

From these results, we realized that mayenite structure and its catalytic activity are strongly connected. Thus, we focused our research to evaluate the influence of different synthetic methods on the mayenite activity for TCE oxidation. Mayenite catalyst was prepared and characterized by using hydrothermal (HA), sol–gel (SG) and ceramic (CR) methods, to obtain materials with different physicochemical properties (crystalline structure, surface area and redox properties) (Intiso et al. 2019a).

The synthesized catalysts have been evaluated for the oxidation of TCE by monitoring the conversion as a function of the temperature. Figure 4 reports the light off curves for a blank experiment, Mayenite HA, SG and CR in absence of water. For blank experiments (thermal oxidation) there was no conversion below 500 °C, while in the presence of mayenite HA, the catalytic activity started at around 200 °C.

As clearly shown in Fig. 4, mayenite prepared by the hydrothermal route showed the best performance in the absence of water. The catalyst  $T_{50}$  was around 350 °C, whilst for mayenite SG and CR was 390 °C and 450 °C, respectively. The conversion yield was found to increase drastically with the temperature, until a total conversion was reached at 550 °C for mayenite HA, where for Mayenite CR and SG only the ~85% conversion of the pollutant was obtained.

The differences in the catalytic activity can be related with the different physicochemical properties of the synthesized materials.

Mayenite prepared by hydrothermal route presented the highest surface area (measured by BET analysis), the highest hydrogen consumption (measured by TPR analysis) and the highest activity. These results are consistent with the

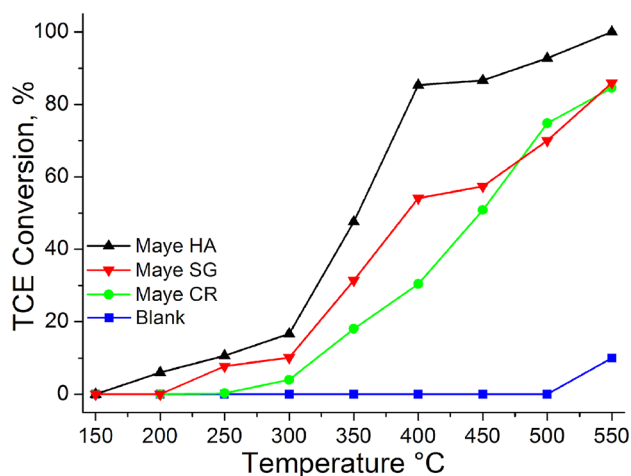


**Fig. 4** TCE conversion in a blank experiment, with mayenite HA, mayenite SG and mayenite CR

existing literature about the fact that activity of the mayenite is related to the presence of  $O^{2-}$  and  $O_2^{2-}$  anions that favor the total oxidation of TCE (Pitkäaho et al. 2011; Joung et al. 2014).

It seems that mayenite synthesized by the hydrothermal method has a good combination of surface area and redox properties that explain the great activity of this material in the TCE oxidation reaction.

The effect of water vapor in the TCE oxidation was also investigated. The results showed that the addition of water to the feed stream did not alter the activity of the mayenite HA.

The selectivity of the reaction was evaluated and the main oxidation products obtained in the trichloroethylene oxidation were found to be carbon dioxide ( $CO_2$ ), carbon monoxide (CO) and hydrogen chloride (HCl). At all the investigated temperatures, chlorine ( $Cl_2$ ) and tetrachloroethylene (PCE) were only detected in trace. Furthermore, a stability test exhibited that after 5 hours of reaction a relevant deactivation of hydrothermal mayenite occurred.

Finally, in order to improve hydrothermal mayenite performances for the TCE oxidation, we developed a new synthetic procedure, based on the addition of different amount of PMMA (10% and 20% w/w) as a soft template agent during mayenite synthesis (Molina and Poncetlet 1998; Solsona et al. 2017). The light off curves of the synthesized mayenites for the TCE oxidation are reported in Fig. 5.

As clearly shown, mayenite 10 was found to be the best catalyst in terms of  $T_{10}$  and  $T_{90}$ . At 200 °C: it was able to degrade (8% of conversion) TCE, while mayenite and mayenite 20 were still inactive. The catalyst  $T_{50}$  and  $T_{90}$  for mayenite 10 were around 350 °C and 440 °C, whilst for mayenite and mayenite 20 being 350/490 °C and 370/450 °C, respectively.

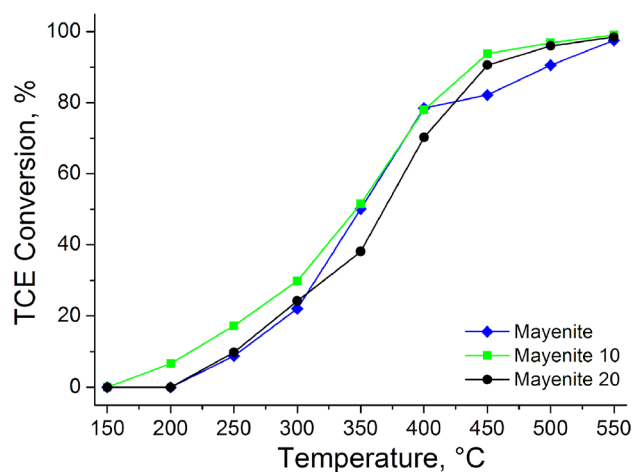


**Fig. 5** TCE conversion for mayenite (rhombus), mayenite 10 (square) and 20 (circle)

As for the studies reported above, the differences among the catalytic activity of the three materials must be related to their different physicochemical properties. In particular, the highest BET surface area and the highest amount of  $O_2^-$  represented the main features determining the best catalytic performances observed for mayenite (Cucciniello et al. 2017a; Intiso et al. 2018).

Thus, in order to prepare an active catalyst for the TCE oxidation, an optimum combination of high surface area and oxidative properties is required. This can be obtained by preparing mayenite-based catalyst by adding PMMA as a soft template agent.

Reaction selectivity was also evaluated and the results showed that the main TCE oxidation products were  $CO_2$ , CO and HCl, confirming our studies described above.

With respect to previous catalytic systems based on noble-metals supported catalysts, mayenite shows several advantages, namely (i) a total conversion of TCE in less harmful  $Cl^-$  and  $CO_2$ , (ii) the presence of free  $O^{2-}$  ions made unnecessary the use of noble and heavy metals, thus reducing the costs and the environmental impact at the end of the material life-cycle and (iii) inexpensive precursors for the material synthesis, such as calcium and aluminium hydroxides.

### 2.3 Mayenite hydrides and electrides

The substitution of the oxygen anions in the nanocages with  $H^-$  promotes the formation of the so-called mayenite hydride (Hayashi et al. 2014b; Jiang et al. 2019). This material has been efficiently used for the reduction of organic compounds. As a matter of fact, selective benzaldehyde reduction to benzyl alcohol was accomplished using Pd dispersed on mayenite ( $Ca_{12}Al_{14}O_{33}$ ) support. Benzaldehyde reduction was observed in  $H_2$  atmosphere (120 °C, 8 atm) and the catalytic performances compared to commercial Pd/C catalyst are superior in terms of selectivity and comparable as activity (Proto et al. 2015). The reduction proceeds also in the presence of sole mayenite as evidence of mayenite hydride activity. The use of mayenite hydrides has been also reported as co-catalyst in hydrogenation reaction. The incorporation of C12A7- $H^-$  increases the reaction rate constants and turnover frequencies of NiW catalysts in hydrodesulfurization of dibenzothiophene. The use of C12A7- $H^-$  promotes the reducibility of NiW catalysts, resulting in higher sulfidation degree and more Ni-W-S species (Liu et al. 2021). Moreover, mayenite was proved to be a cost-effective material, in the hydride state ( $H^-$ ), for hydrogen storage and transportation (Visbal et al. 2021). The authors described the hydrogen desorption by the reaction of mayenite with water. This reaction favors the desorption of hydride ions trapped in the structure. This recently published result is of high interest also in the light of potential application of

mayenite (100% recyclable because the cage structure can be recovered by heat treatment after hydrogen desorption) in portable devices.

A class of extraordinary interest is represented by electride. Electrides are materials in which electrons behave as anions. Mayenite electrides were reported by Hosono and coworkers in 2003 and that they are stable in air at room temperature exhibiting metallic characteristics (ionic conductivity  $1500\text{ S cm}^{-1}$ ) and a low work function of 2.4 eV (Matsuishi et al. 2003). One of the most investigated applications of these electrides consists in the use as active support, mainly for Ru, for ammonia synthesis from  $N_2$  and  $H_2$ . High surface area ( $20\text{ m}^2\text{ g}^{-1}$ ) electrides are produced through mayenite reduction with  $CaH_2$ . Ru/HT-C12A7: $e^-$  catalyst shows high productivity in the  $NH_3$  synthesis with a maximum ( $2.4\text{ mmol g}^{-1}\text{ h}^{-1}$ ) at 1173 K, which is superior to that for conventional Ru catalysts (Inoue et al. 2014). The electron-donating ability of HT-C12A7: $e^-$  is able to promote  $N_2$  dissociation on the Ru catalyst. Mayenite electrides have been also reported as active materials in (i) the pinacol coupling reaction in aqueous media (Buchammagari et al. 2007), (ii) the selective hydrogenation reactions, in combination with Ru-Fe nanoalloy, of  $\alpha$ ,  $\beta$ -unsaturated aldehydes to the corresponding unsaturated alcohols, and (iii) Suzuki cross-coupling reaction (Ye et al. 2016).

### 3 Other relevant applications of mayenite and its derivatives

Mayenite and mayenite-based materials have been extensively used in the past for a wide range of applications. In 2008, Ruzsak et al. studied the high-temperature decomposition of nitrous oxide,  $N_2O$ , over mayenite (Ruzsak et al. 2008). This application is very interesting because in the nitric acid plants,  $N_2O$  is an undesirable by-product and two types of  $N_2O$  removal technologies are available on the market: a non-catalytic one and a catalytic one. The non-catalytic technique involves the thermal destruction of  $N_2O$  and mayenite support can be used in this context. Authors show an appreciable conversion of  $N_2O$  above 850 K and upon reaching the process temperature of 1150 K the decomposition of nitrous oxide achieved ca. 90%. From a mechanistic point of view, for the  $N_2O$  decomposition over oxide catalysts not containing transition metal ions the anionic redox mechanism initiated by the oxygen atom transfer was proposed. In this context the peculiar feature of mayenite, with its large capacity for storage of the subsurface oxygen species, opens two interesting mechanistic pathways: superficial recombination of surface peroxy ions and interfacial recombination of surface peroxy with cage and surface oxygen species.

CaO/mayenite-based materials have been also used as active sorbents for atmospheric pollutants in active and passive samplers (Guerranti et al. 2016). The first use of mayenite for this application was reported in 2012 in combination with CaO for CO<sub>2</sub> passive sampling. Mayenite was used to increase the sorbent particle size in order to inhibit the sorbent leaking from the device (Cucciniello et al. 2012). CaO/Ca<sub>12</sub>Al<sub>14</sub>O<sub>33</sub> 75:25 w/w sorbent has been also used for passive sampling of atmospheric carbon dioxide for δ<sup>13</sup>C analysis in both indoor and outdoor places (Proto et al. 2014; Pironti et al. 2021). Successively, mayenite-based sorbents were employed as active substrates for NO<sub>x</sub> sampling. Herein, various CaO/Mayenite substrates having different weight ratio (w/w) composition were prepared and their reactivity towards NO and NO<sub>2</sub> was evaluated. FTIR and ion chromatography analysis showed a good capacity of both NO and NO<sub>2</sub> sorption through the formation of nitrates and nitrites species on the sorption surface (Cucciniello et al. 2013). The as-obtained results have further been applied for the preparation of a new NO<sub>x</sub> active sampler based on mayenite as sorbent (Cucciniello et al. 2017b).

## 4 Conclusions

In conclusion, mayenite shows interesting applications as a consequence of its peculiar chemical-physics properties. The main features of mayenite have been evaluated in oxidation reactions, especially for environmental pollutants degradation. Mayenite acts as active catalyst due to the presence of oxygen anions into the nanocages that are able to oxidize organic and inorganic compounds. Mayenite derivatives, obtained through the anion exchange, also exhibited excellent performances as both active and reactive support or as catalyst in several important processes.

**Acknowledgements** R.C. wants to thank the Accademia Nazionale dei Lincei for “Alfredo Di Braccio 2020” award.

**Funding** Open access funding provided by Università degli Studi di Salerno within the CRUI-CARE Agreement.

**Open Access** This article is licensed under a Creative Commons Attribution 4.0 International License, which permits use, sharing, adaptation, distribution and reproduction in any medium or format, as long as you give appropriate credit to the original author(s) and the source, provide a link to the Creative Commons licence, and indicate if changes were made. The images or other third party material in this article are included in the article's Creative Commons licence, unless indicated otherwise in a credit line to the material. If material is not included in the article's Creative Commons licence and your intended use is not permitted by statutory regulation or exceeds the permitted use, you will need to obtain permission directly from the copyright holder. To view a copy of this licence, visit <http://creativecommons.org/licenses/by/4.0/>.

## References

- Amann M, Lutz M (2000) The revision of the air quality legislation in the European Union related to ground-level ozone. *J Hazard Mater* 78:41–62. [https://doi.org/10.1016/S0304-3894\(00\)00216-8](https://doi.org/10.1016/S0304-3894(00)00216-8)
- Aranzabal A, Romero-Sáez M, Elizundia U et al (2012) Deactivation of H-zeolites during catalytic oxidation of trichloroethylene. *J Catal* 296:165–174. <https://doi.org/10.1016/j.jcat.2012.09.012>
- Aranzabal A, Pereda-Ayo B, González-Marcos M et al (2014) State of the art in catalytic oxidation of chlorinated volatile organic compounds. *Chem Pap* 68:1169–1186. <https://doi.org/10.2478/s11696-013-0505-7>
- Blanch-Raga N, Palomares AE, Martínez-Triguero J et al (2014) The oxidation of trichloroethylene over different mixed oxides derived from hydrocalcites. *Appl Catal B Environ* 160:129–134
- Blanch-Raga N, Palomares AE, Martínez-Triguero J, Valencia S (2016) Cu and Co modified beta zeolite catalysts for the trichloroethylene oxidation. *Appl Catal B Environ* 187:90–97. <https://doi.org/10.1016/j.apcatb.2016.01.029>
- Buchamagari H, Toda Y, Hirano M et al (2007) Room temperature-stable electride as a synthetic organic reagent: application to pinacol coupling reaction in aqueous media. *Org Lett* 9:4287–4289. <https://doi.org/10.1021/ol701885p>
- Cucciniello R, Proto A, Alfano D, Motta O (2012) Synthesis, characterization and field evaluation of a new calcium-based CO<sub>2</sub> absorbent for radial diffusive sampler. *Atmos Environ* 60:82–87. <https://doi.org/10.1016/j.atmosenv.2012.06.023>
- Cucciniello R, Proto A, Rossi F, Motta O (2013) Mayenite based supports for atmospheric NO<sub>x</sub> sampling. *Atmos Environ* 79:666–671. <https://doi.org/10.1016/j.atmosenv.2013.07.065>
- Cucciniello R, Intiso A, Castiglione S et al (2017a) Total oxidation of trichloroethylene over mayenite (Ca<sub>12</sub>Al<sub>14</sub>O<sub>33</sub>) catalyst. *Appl Catal B Environ* 204:167–172. <https://doi.org/10.1016/j.apcatb.2016.11.035>
- Cucciniello R, Proto A, La Femina R et al (2017b) A new sorbent tube for atmospheric NO<sub>x</sub> determination by active sampling. *Talanta* 164:403–406. <https://doi.org/10.1016/j.talanta.2016.12.006>
- Cucciniello R, Intiso A, Siciliano T et al (2019) Oxidative degradation of trichloroethylene over Fe<sub>2</sub>O<sub>3</sub>-doped mayenite: chlorine poisoning mitigation and improved catalytic performance. *Catalysts* 9:747. <https://doi.org/10.3390/catal9090747>
- Da Fumo A, Morelli MR, Segadães AM (1996) Combustion synthesis of calcium aluminates. *Mater Res Bull* 31:1243–1255. [https://doi.org/10.1016/0025-5408\(96\)00112-2](https://doi.org/10.1016/0025-5408(96)00112-2)
- Divakar D, Romero-Sáez M, Pereda-Ayo B et al (2011) Catalytic oxidation of trichloroethylene over Fe-zeolites. *Catal Today* 176:357–360. <https://doi.org/10.1016/j.cattod.2010.11.065>
- Dong Y, Hosono H, Hayashi K (2013) Formation and quantification of peroxide anions in nanocages of 12CaO·7Al<sub>2</sub>O<sub>3</sub>. *RSC Adv* 3:18311–18316. <https://doi.org/10.1039/C3RA42521E>
- Eufinger J-P, Schmidt A, Lerch M, Janek J (2015) Novel anion conductors—conductivity, thermodynamic stability and hydration of anion-substituted mayenite-type cage compounds C12A7: X (X = O, OH, Cl, F, CN, S, N). *Phys Chem Chem Phys* 17:6844–6857. <https://doi.org/10.1039/C4CP05442C>
- Fujita S, Nakano H, Suzuki K et al (2006) Oxidative destruction of hydrocarbons on Ca<sub>12</sub>Al<sub>14-x</sub>Si<sub>x</sub>O<sub>33</sub>+0.5x (0 ≤ x ≤ 4) with radical oxygen occluded in nanopores. *Catal Lett* 106:139–143. <https://doi.org/10.1007/s10562-005-9621-5>
- Gołabek K, Palomares AE, Martínez-Triguero J et al (2019) Ce-modified zeolite BEA catalysts for the trichloroethylene oxidation. The role of the different and necessary active sites. *Appl Catal B Environ* 259:118022. <https://doi.org/10.1016/j.apcatb.2019.118022>



- Guerranti C, Benetti F, Cucciniello R et al (2016) Pollutants monitoring and air quality evaluation in a confined environment: the ‘Majesty’ of Ambrogio Lorenzetti in the St. Augustine Church in Siena (Italy). *Atmospheric Pollut Res* 7:754–761. <https://doi.org/10.1016/j.apr.2016.04.002>
- Hayashi K, Hirano M, Matsuishi S, Hosono H (2002a) Microporous crystal  $12\text{CaO}\cdot 7\text{Al}_2\text{O}_3$  encaging abundant O<sup>-</sup> radicals. *J Am Chem Soc* 124:738–739. <https://doi.org/10.1021/ja016112n>
- Hayashi K, Matsuishi S, Kamiya T et al (2002b) Light-induced conversion of an insulating refractory oxide into a persistent electronic conductor. *Nature* 419:462–465. <https://doi.org/10.1038/nature01053>
- Hayashi K, Hirano M, Hosono H (2005) Thermodynamics and kinetics of hydroxide ion formation in  $12\text{CaO}\cdot 7\text{Al}_2\text{O}_3$ . *J Phys Chem B* 109:11900–11906. <https://doi.org/10.1021/jp050807j>
- Hayashi K, Sushko PV, Ramo DM et al (2007) Nanoporous crystal  $12\text{CaO}\cdot 7\text{Al}_2\text{O}_3$ : a playground for studies of ultraviolet optical absorption of negative ions. *J Phys Chem B* 111:1946–1956. <https://doi.org/10.1021/jp065793b>
- Hayashi F, Tomota Y, Kitano M et al (2014a)  $\text{NH}_2^-$  dianion entrapped in a nanoporous  $12\text{CaO}\cdot 7\text{Al}_2\text{O}_3$  crystal by ammonothermal treatment: reaction pathways, dynamics, and chemical stability. *J Am Chem Soc* 136:11698–11706. <https://doi.org/10.1021/ja504185m>
- Hayashi K, Sushko PV, Hashimoto Y et al (2014b) Hydride ions in oxide hosts hidden by hydroxide ions. *Nat Commun* 5:3515. <https://doi.org/10.1038/ncomms4515>
- Heck RM, Farrauto RJ, Gulati ST (2012) Catalytic air pollution control: commercial technology, 3rd edn. John Wiley & Sons Inc, Hoboken
- IARC Working Group on the Evaluation of Carcinogenic Risks to Humans (2014) Trichloroethylene, tetrachloroethylene, and some other chlorinated agents. *IARC Monogr Eval Carcinog Risks Hum* 106:1–512
- Inoue Y, Kitano M, Kim S-W et al (2014) Highly Dispersed Ru on Electride  $[\text{Ca}_{24}\text{Al}_{28}\text{O}_{64}]^{4+}(e^-)_4$  as a catalyst for ammonia synthesis. *ACS Catal* 4:674–680. <https://doi.org/10.1021/cs401044a>
- Intiso A, Cucciniello R, Castiglione S et al (2018) Environmental application of extra-framework oxygen anions in the nano-cages of mayenite. *Advances in Bionanomaterials*. Springer, Cham, pp 131–139
- Intiso A, Martinez-Triguero J, Cucciniello R et al (2019a) Influence of the synthesis method on the catalytic activity of mayenite for the oxidation of gas-phase trichloroethylene. *Sci Rep* 9:425. <https://doi.org/10.1038/s41598-018-36708-2>
- Intiso A, Martinez-Triguero J, Cucciniello R et al (2019b) A novel synthetic route to prepare high surface area mayenite catalyst for TCE oxidation. *Catalysts* 9:27. <https://doi.org/10.3390/catal9010027>
- Jiang D, Zhao Z, Mu S et al (2019) Insights into the dynamic hydrogenation of mayenite  $[\text{Ca}_{24}\text{Al}_{28}\text{O}_{64}]^{4+}(\text{O}_2^-)_2$ : mixed ionic and electronic conduction within the sub-nanometer cages. *Int J Hydrog Energy* 44:18360–18371. <https://doi.org/10.1016/j.ijhydene.2019.05.094>
- Joung H-J, Kim J-H, Oh J-S et al (2014) Catalytic oxidation of VOCs over CNT-supported platinum nanoparticles. *Appl Surf Sci* 290:267–273. <https://doi.org/10.1016/j.apsusc.2013.11.066>
- Kitano M, Inoue Y, Yamazaki Y et al (2012) Ammonia synthesis using a stable electride as an electron donor and reversible hydrogen store. *Nat Chem* 4:934–940. <https://doi.org/10.1038/NCHEM.1476>
- Lacerda M, Irvine JTS, Glasser FP, West AR (1988) High oxide ion conductivity in  $\text{Ca}_{12}\text{Al}_{14}\text{O}_{33}$ . *Nature* 332:525–526. <https://doi.org/10.1038/332525a0>
- Li C, Hirabayashi D, Suzuki K (2009) A crucial role of  $\text{O}_2^-$  and  $\text{O}_2^{2-}$  on mayenite structure for biomass tar steam reforming over  $\text{Ni}/\text{Ca}_{12}\text{Al}_{14}\text{O}_{33}$ . *Appl Catal B Environ* 88:351–360. <https://doi.org/10.1016/j.apcatb.2008.11.004>
- Li C, Hirabayashi D, Suzuki K (2011) Synthesis of higher surface area mayenite by hydrothermal method. *Mater Res Bull* 46:1307–1310. <https://doi.org/10.1016/j.materresbull.2011.03.023>
- Liotta LF (2010) Catalytic oxidation of volatile organic compounds on supported noble metals. *Appl Catal B Environ* 100:403–412. <https://doi.org/10.1016/j.apcatb.2010.08.023>
- Liu X, Li L, Sun H et al (2021) NiW catalyst modified with  $\text{C}_{12}\text{A}_7\text{-H}^-$  and its promotion to hydrogenation selectivity of hydrodesulfurization. *Fuel* 290:120037. <https://doi.org/10.1016/j.fuel.2020.120037>
- López-Fonseca R, Gutiérrez-Ortiz JI, González-Velasco JR (2004) Catalytic combustion of chlorinated hydrocarbons over H-BETA and PdO/H-BETA zeolite catalysts. *Appl Catal Gen* 271:39–46. <https://doi.org/10.1016/j.apcata.2004.02.044>
- Manera C, Perondi D, Barbieri RA et al (2020) Ultrasonication-promoted synthesis of Ni/mayenite for catalytic reforming of biomass tar. *Ultrason Sonochem* 67:105165. <https://doi.org/10.1016/j.ultsonch.2020.105165>
- Matsuishi S, Toda Y, Miyakawa M et al (2003) High-density electron anions in a nanoporous single crystal:  $[\text{Ca}_{24}\text{Al}_{28}\text{O}_{64}]^{4+}(4e^-)$ . *Science* 301:626–629. <https://doi.org/10.1126/science.1083842>
- Meza-Trujillo I, Devred F, Gaigneaux EM (2019) Production of high surface area mayenite ( $\text{C}_{12}\text{A}_7$ ) via an assisted solution combustion synthesis (SCS) toward catalytic soot oxidation. *Mater Res Bull* 119:110542. <https://doi.org/10.1016/j.materresbull.2019.110542>
- Molina R, Poncet G (1998)  $\alpha$ -Alumina-supported nickel catalysts prepared from nickel acetylacetonate: a TPR study. *J Catal* 173:257–267. <https://doi.org/10.1006/jcat.1997.1931>
- Pironti C, Ricciardi M, Proto A et al (2021) New analytical approach to monitoring air quality in historical monuments through the isotopic ratio of  $\text{CO}_2$ . *Environ Sci Pollut Res*. <https://doi.org/10.1007/s11356-020-12215-8>
- Pitkääho S, Ojala S, Maunula T et al (2011) Oxidation of dichloromethane and perchloroethylene as single compounds and in mixtures. *Appl Catal B Environ* 102:395–403. <https://doi.org/10.1016/j.apcatb.2010.12.011>
- Proto A, Cucciniello R, Rossi F, Motta O (2014) Stable carbon isotope ratio in atmospheric  $\text{CO}_2$  collected by new diffusive devices. *Environ Sci Pollut Res* 21:3182–3186. <https://doi.org/10.1007/s11356-013-2369-3>
- Proto A, Cucciniello R, Genga A, Capacchione C (2015) A study on the catalytic hydrogenation of aldehydes using mayenite as active support for palladium. *Catal Commun* 68:41–45. <https://doi.org/10.1016/j.catcom.2015.04.028>
- Raab B, Poellmann H (2011) Heat flow calorimetry and SEM investigations to characterize the hydration at different temperatures of different  $12\text{CaO}\cdot\text{Al}_2\text{O}_3$  ( $\text{C}_{12}\text{A}_7$ ) samples synthesized by solid state reaction, polymer precursor process and glycine nitrate process. *Thermochim Acta* 513:106–111. <https://doi.org/10.1016/j.tca.2010.11.019>
- Rashad MM, Mostafa AG, Rayan DA (2016) Structural and optical properties of nanocrystalline mayenite  $\text{Ca}_{12}\text{Al}_{14}\text{O}_{33}$  powders synthesized using a novel route. *J Mater Sci Mater Electron* 27:2614–2623. <https://doi.org/10.1007/s10854-015-4067-z>
- Romero-Sáez M, Divakar D, Aranzabal A et al (2016) Catalytic oxidation of trichloroethylene over Fe-ZSM-5: Influence of the preparation method on the iron species and the catalytic behavior. *Appl Catal B Environ* 180:210–218. <https://doi.org/10.1016/j.apcatb.2015.06.027>
- Rossi F, Cucciniello R, Intiso A et al (2015) Determination of the trichloroethylene diffusion coefficient in water. *AICHE J* 61:3511–3515. <https://doi.org/10.1002/aic.14861>

- Ruszek M, Witkowski S, Sojka Z (2007) EPR and Raman investigations into anionic redox chemistry of nanoporous  $12\text{CaO}\cdot 7\text{Al}_2\text{O}_3$  interacting with  $\text{O}_2$ ,  $\text{H}_2$  and  $\text{N}_2\text{O}$ . *Res Chem Intermed* 33:689–703. <https://doi.org/10.1163/156856707782169435>
- Ruszek M, Inger M, Witkowski S et al (2008) Selective N(2)O removal from the process gas of nitric acid plants over ceramic  $12\text{CaO}$  center dot  $7\text{Al}_2\text{O}_3$  catalyst. *Catal Lett* 126:72–77. <https://doi.org/10.1007/s10562-008-9619-x>
- Scaccia S, Della Seta L, Mirabile Gattia D, Vanga G (2021) Catalytic performance of Ni/CaO- $\text{Ca}_{12}\text{Al}_{14}\text{O}_{33}$  catalyst in the green synthesis gas production via  $\text{CO}_2$  reforming of  $\text{CH}_4$ . *J CO2 Util* 45:101447. <https://doi.org/10.1016/j.jcou.2021.101447>
- Schmidt A, Lerch M, Eufinger J-P et al (2014) Chlorine ion mobility in Cl-mayenite ( $\text{Ca}_{12}\text{Al}_{14}\text{O}_{32}\text{Cl}_2$ ): an investigation combining high-temperature neutron powder diffraction, impedance spectroscopy and quantum-chemical calculations. *Solid State Ion* 254:48–58. <https://doi.org/10.1016/j.ssi.2013.10.042>
- Scirè S, Liotta LF (2012) Supported gold catalysts for the total oxidation of volatile organic compounds. *Appl Catal B Environ* 125:222–246. <https://doi.org/10.1016/j.apcatb.2012.05.047>
- Solsona B, Sanchis R, Dejoz AM et al (2017) Total oxidation of propane using  $\text{CeO}_2$  and  $\text{CuO-CeO}_2$  catalysts prepared using templates of different nature. *Catalysts* 7:96
- Teusner M, De Souza RA, Krause H et al (2015) Oxygen diffusion in mayenite. *J Phys Chem C* 119:9721–9727
- Teusner M, De Souza RA, Krause H et al (2016) Oxygen transport in undoped and doped mayenite. *Solid State Ion* 284:25–27. <https://doi.org/10.1016/j.ssi.2015.11.024>
- Tomatis M, Xu H-H, He J, Zhang X-D (2016) Recent development of catalysts for removal of volatile organic compounds in flue gas by combustion: a review. *J Chem* 2016:e8324826. <https://doi.org/10.1155/2016/8324826>
- Ude SN, Rawn CJ, Peascoe RA et al (2014) High temperature X-ray studies of mayenite synthesized using the citrate sol–gel method. *Ceram Int* 40:1117–1123. <https://doi.org/10.1016/j.ceramint.2013.06.112>
- Vernoux P, Lizarraga L, Tsampas MN et al (2013) Ionically conducting ceramics as active catalyst supports. *Chem Rev* 113:8192–8260. <https://doi.org/10.1021/cr4000336>
- Visbal H, Omura T, Nagashima K et al (2021) Exploring the capability of mayenite ( $12\text{CaO}\cdot 7\text{Al}_2\text{O}_3$ ) as hydrogen storage material. *Sci Rep* 11:6278. <https://doi.org/10.1038/s41598-021-85540-8>
- Wang X, He Y, Xu T et al (2020)  $\text{CO}_2$  sorption-enhanced steam reforming of phenol using Ni-M/CaO- $\text{Ca}_{12}\text{Al}_{14}\text{O}_{33}$  (M = Cu Co, and Ce) as catalytic sorbents. *Chem Eng J* 393:124769. <https://doi.org/10.1016/j.cej.2020.124769>
- Yang S, Kondo JN, Hayashi K et al (2004) Partial oxidation of methane to syngas over promoted C12A7. *Appl Catal Gen* 277:239–246. <https://doi.org/10.1016/j.apcata.2004.09.030>
- Ye T-N, Li J, Kitano M et al (2016) Electronic interactions between a stable electrode and a nano-alloy control the chemoselective reduction reaction. *Chem Sci* 7:5969–5975. <https://doi.org/10.1039/C6SC01864E>
- Zamboni I, Courson C, Niznansky D, Kiennemann A (2014) Simultaneous catalytic  $\text{H}_2$  production and  $\text{CO}_2$  capture in steam reforming of toluene as tar model compound from biomass gasification. *Appl Catal B Environ* 145:63–72. <https://doi.org/10.1016/j.apcatb.2013.02.046>
- Zamboni I, Zimmermann Y, Kiennemann A, Courson C (2015) Improvement of steam reforming of toluene by  $\text{CO}_2$  capture using Fe/CaO- $\text{Ca}_{12}\text{Al}_{14}\text{O}_{33}$  bi-functional materials. *Int J Hydrog Energy* 40:5297–5304. <https://doi.org/10.1016/j.ijhydene.2015.01.065>
- Zhang Z, Kong Z, Liu H, Chen Y (2014) Mayenite supported perovskite monoliths for catalytic combustion of methyl methacrylate. *Front Chem Sci Eng* 8:87–94. <https://doi.org/10.1007/s11705-014-1410-5>

**Publisher's Note** Springer Nature remains neutral with regard to jurisdictional claims in published maps and institutional affiliations.